INFECTION AND IMMUNITY, May 2003, p. 2970–2975 Vol. 71, No. 5
0019-9567/03/$08.00+0 DOI: 10.1128/IAI.71.5.2970–2975.2003

Structural and Functional Cellular Changes Induced by *Burkholderia pseudomallei* Rhamnolipid

S. Häußler,[1] M. Rohde,[2] N. von Neuhoff,[3] M. Nimtz,[2] and I. Steinmetz[1]*

Institute of Medical Microbiology[1] and Institute of Cell and Molecular Pathology,[3] Hannover Medical School, Hannover, and German Research Centre for Biotechnology, Braunschweig,[2] Germany

Received 26 June 2002/Returned for modification 17 October 2002/Accepted 13 January 2003

In this study we report that extracellular *Burkholderia pseudomallei* rhamnolipid induced cytopathic changes characterized by retraction, rounding up, and, finally, detachment in phagocytic and nonphagocytic cell lines. These changes were due to a progressive reorganization of the F-actin network resulting in impaired cell cycle progression and a reduced phagocytic function of macrophages.

The saprophytic bacterium *Burkholderia pseudomallei* is the causative agent of melioidosis, an infectious disease of humans and animals. Although the pathogen is widely found in soil and surface water throughout the tropics, the incidence of melioidosis is particularly high in southern Asia and northern Australia (5, 6, 8). Clinical melioidosis in children frequently presents itself as suppurative parotidis (7). The majority of adult patients develop acute pulmonary or septicemic illness, with high mortality rates (6), or subacute melioidosis, characterized by multiple-abscess formation. The disease is difficult to treat, and even under appropriate antimicrobial therapy protracted clinical courses occur (22). Although melioidosis is increasingly recognized as an emerging infection in the regions where the disease is endemic (17), only a few studies of the molecular basis of the host-pathogen interaction in melioidosis have been carried out (3). Bacterial components which have clearly been shown to be required for virulence are an endotoxin-derived O polysaccharide (9) and a capsular polysaccharide (20). The potential role of other secreted or cell-associated *B. pseudomallei* antigens in the pathogenesis of melioidosis remains to be elucidated. We have recently identified a *B. pseudomallei* rhamnolipid, composed of two molecules of rhamnose and two molecules of β-hydroxytetradecanoic acids (14), which at high concentrations exhibited a time- and dose-dependent cytotoxicity against nonphagocytic and phagocytic cell lines, likely caused by a detergent-like activity. The results presented in this study show that (i) low concentrations of the *B. pseudomallei* rhamnolipid induced a cytopathic effect characterized by changes in cell morphology due to modifications of the cytoskeleton organization without affecting cell viability, (ii) cells treated with rhamnolipid exhibited an impaired cell cycle progression, and (iii) rhamnolipid-treated, tissue-cultured macrophages internalized fewer viable *B. pseudomallei* bacteria.

Preparation of *B. pseudomallei* rhamnolipid. *B. pseudomallei* rhamnolipid was purified from culture supernatants as described previously (14) with modifications. Briefly, *B. pseudomallei* ATCC 7431, obtained from the American Type Culture Collection, was grown on 20 Columbia agar plates overnight at 37°C and resuspended in 2 liters of 0.15 M NaCl plus 4% (vol/vol) glycerol (pH 7.0). After incubation at 37°C with shaking for 6 days, the culture was centrifuged for 30 min at 5,000 × *g*. The supernatant was heat inactivated and extracted with 1 liter of dichloromethane (Merck, Darmstadt, Germany). The lower dichloromethane phase was evaporated, and the residue was dissolved in 0.1% (vol/vol) trifluoroacetic acid (Sigma, St. Louis, Mo.). The material was further purified by fast-performance liquid chromatography as described previously (14). The lyophilized material was dissolved in distilled water and further analyzed by mass spectrometry to assess the purity and quantity of *B. pseudomallei* rhamnolipid as described previously (14). Lipopolysaccharide (LPS) determinations by the *Limulus* amoebocyte lysate assay (21) revealed LPS contaminations of ~0.07% in the *B. pseudomallei* rhamnolipid preparations used in this study.

Cell culture and cytotoxicity assay. The cell lines J774.A1 and A549 used in this study were obtained from the German Collection of Microorganisms and Cell Cultures in Braunschweig. The PtK_2 cell line was obtained from the American Type Culture Collection. Since PtK2 cells are particularly suitable for the analysis of the cytoskeletal organization, these cells were used to label filamentous actin, vimentin, and tubulin. All cell lines were grown in Dulbecco's modified Eagle medium containing 10% fetal calf serum at 37°C in an atmosphere with 5% CO_2. For the analysis of morphological changes, A549 and PtK_2 cells were grown to confluence and treated with trypsin-EDTA, while J774.A1 cells were harvested with the use of a cell scraper. The cells were diluted in fresh medium, seeded onto glass slides in a 24-well tissue culture plate at a concentration of 5×10^4 cells/well in 1 ml of medium, and incubated for 24 h. Because albumin has been shown to interfere with rhamnolipid activity (14), rhamnolipid was added to the cells in serum-free medium (Panserin 501). A549 and PtK_2 cells were exposed to ~15 μg of rhamnolipid per ml, while the J774.A1 cell line was exposed to ~7.5 μg/ml for the time intervals indicated in the legend to Fig. 1. The rhamnolipid concentrations used in this study exhibited no immediate effect on cell viability as determined by trypan blue exclusion. *B. pseudomallei* LPS-containing bacterial extracts (21) were used as negative controls.

* Corresponding author. Mailing address: Medical Microbiology, Hannover Medical School, Carl-Neuberg-Str. 1, 30625 Hannover, Germany. Phone: 0511-532-4352. Fax: 0511-532-4366. E-mail: Steinmetz.Ivo@MH-Hannover.DE.

Scanning electron microscopy. For the analysis of rhamnolipid-induced morphological changes, the cells were visualized by scanning electron microscopy. A549, PtK_2, and J774.A1 cells were grown on glass slides and exposed to rhamnolipid as described above. At given time intervals, the cells were washed twice with phosphate-buffered saline, pH 7.4 (PBS), and fixed in 3% (vol/vol) glutaraldehyde and 5% (wt/vol) paraformaldehyde in PBS for 1 h on ice. After being washed with Tris-EDTA buffer (10 mM Tris, 2 mM EDTA [pH 6.9]), the samples were dehydrated with acetone on ice and further dried by application of the critical-point drying method with liquid CO_2. The samples were then sputter coated with a thin gold film (approximately 10 nm in thickness) before examination in a Zeiss DSM982 Gemini field emission scanning electron microscope at an acceleration voltage of 5 kV.

Fluorescence microscopy of the cytoskeleton. To label F-actin, control and rhamnolipid-treated PtK_2 cells grown on glass slides as described above were washed twice with PBS at the time points indicated in the legend to Fig. 2, fixed with 3% paraformaldehyde in PBS for 20 min at room temperature, washed three times with PBS, and incubated with 10 mM NH_4Cl-PBS for 10 min. After being washed twice with PBS, the cells were permeabilized with 0.1% Triton X-100 in PBS for 5 min and further incubated with 0.5% bovine serum albumin (BSA) in PBS for 30 min. The cells were then treated for 30 min with a 10-U/ml concentration of Alexa Fluor 488 dye-conjugated phalloidin (Molecular Probes, Eugene, Oreg.) in PBS, washed three times with PBS, and mounted with Fluoprep medium (Biomerieux, Marcy l'Etoile, France).

To visualize the intermediate filaments, PtK_2 cells were fixed, permeabilized, and treated with BSA as described above. After incubation for 30 min with mouse antivimentin immunoglobulin G (IgG) antibody (15), the cells were washed three times with PBS and exposed to goat anti-mouse fluorescein isothiocyanate-conjugated immunoglobulin (Dianova, Hamburg, Germany) for 30 min, washed with PBS, and then mounted. To label the microtubule network, the cells were fixed in −20°C methanol for 4 min, treated with BSA, washed with PBS, and incubated for 30 min with mouse antitubulin IgG antibody (N357; Amersham, Little Chalfont, Buckinghamshire, United Kingdom), as described by Blose et al. (2). After the cells were washed three times with PBS, they were exposed to fluorescein isothiocyanate-conjugated goat anti-mouse IgG as described above and mounted. The slides were examined and photographed with a fluorescence microscope (model DM IRB/E; Leica, Wetzlar, Germany).

Flow cytometry for cell cycle analysis. Approximately 4×10^6 A549 and J774.A1 cells were grown overnight in cell culture flasks in a volume of 15 ml. The next day, the medium containing the A549 cells was replaced by 5 ml of serum-free medium containing either 1 μg of rhamnolipid per ml or no rhamnolipid, whereas the J774.A1 cells were grown in medium containing 10% fetal calf serum and either 1 μg of rhamnolipid per ml or no rhamnolipid. After 24 h, the adherent cells were harvested with the aid of a cell scraper and the cell nuclei were isolated and stained with a cycleTEST PLUS DNA reagent kit (Becton Dickinson). The test principle is based on the measurement of the DNA content of cell nuclei, which varies in the different phases of the cell cycle and can be detected by using a fluorescent dye. The nuclei were analyzed with a FACSCalibur (Becton Dickinson Immunocytometry Systems, San Jose, Calif.) and Cell Quest software version 3.3. The resulting fluorescence histograms were further analyzed with ModFit software version 3.0. All experiments were performed on three separate occasions.

Phagocytosis assay. *B. pseudomallei* strain E8 was obtained from N. J. White (Wellcome-Mahidol-Oxford Tropical Medicine Research Programme, Bangkok, Thailand) and used to analyze bacterial internalization in the mouse macrophage cell line J774.A1. Cells (1×10^4) were grown overnight in 96-well tissue culture plates (200 μl/well), stimulated for 24 h with gamma interferon (300 U/ml), and treated with 50 μl of serum-free medium containing either ~15 μg of rhamnolipid per ml or no rhamnolipid. After 3 h of rhamnolipid exposure, the *B. pseudomallei* strain E8 was resuspended in serum-free medium and the bacteria were added at a multiplicity of infection of 10 bacteria per cell in a volume of 50 μl/well. After a 30-min incubation at 37°C, the cells were washed three times with PBS and lysed with 1% Triton X-100 in PBS. For CFU determination, serially diluted samples were plated onto Mueller-Hinton agar plates. The internalization assay was performed twice in triplicate.

***B. pseudomallei* rhamnolipid induces morphological cellular changes.** We have previously shown that *B. pseudomallei* rhamnolipid, which is secreted in large amounts when bacterial cells are cultured at high cell densities, exerts a cytotoxic effect on eukaryotic cells (14), probably by directly perturbing cell membranes at concentrations in the range of micrograms per milliliter. In this study we investigated the effect of toxin concentrations in the range of micrograms per milliliter; no immediate effect on cell viability occurred but marked morphological alterations were observed.

Figure 1 shows the morphological alterations of various cell lines induced by *B. pseudomallei* rhamnolipid. Besides promoting the progressive rounding up and detachment of J774.A1 cells, rhamnolipid promoted the spreading of these cells at 6 h of rhamnolipid exposure (compare Fig. 1A, which shows the control, and B). At later time points (12 h), lamellopodia and vial formation seemed to be eliminated in rhamnolipid-treated cells (Fig. 1C). Rhamnolipid exposure of PtK_2 and A549 cells also led to a retraction of the cells. Within 6 h, individual cells began to be discernible (Fig. 1E and H), and prolonged rhamnolipid exposure led to progressive retraction and detachment (Fig. 1F and I). After 24 h, most of the rhamnolipid-treated cells were detached from the surface (data not shown). The cellular morphological alterations were not specific for *B. pseudomallei* rhamnolipid, as the described effects could also be observed after exposure to the structurally very similar *Pseudomonas aeruginosa* rhamnolipid (data not shown), which is composed of two molecules of rhamnose and two molecules of β-hydroxydecanoic acids (19).

Intoxication of PtK_2 cells with *B. pseudomallei* rhamnolipid results in a reorganization of the actin cytoskeleton. The cytoskeletal organization of the PtK_2 cell line after exposure to rhamnolipid was analyzed by labeling F-actin, vimentin, and tubulin. Initial changes in the cytoskeleton organization occurred within 6 h and could be visualized by F-actin staining (Fig. 2A). In contrast to what was seen in control cells, where many stress fibers ended at cell-to-cell contacts, only a very few stress fibers were seen traversing the cytoplasm in cells treated

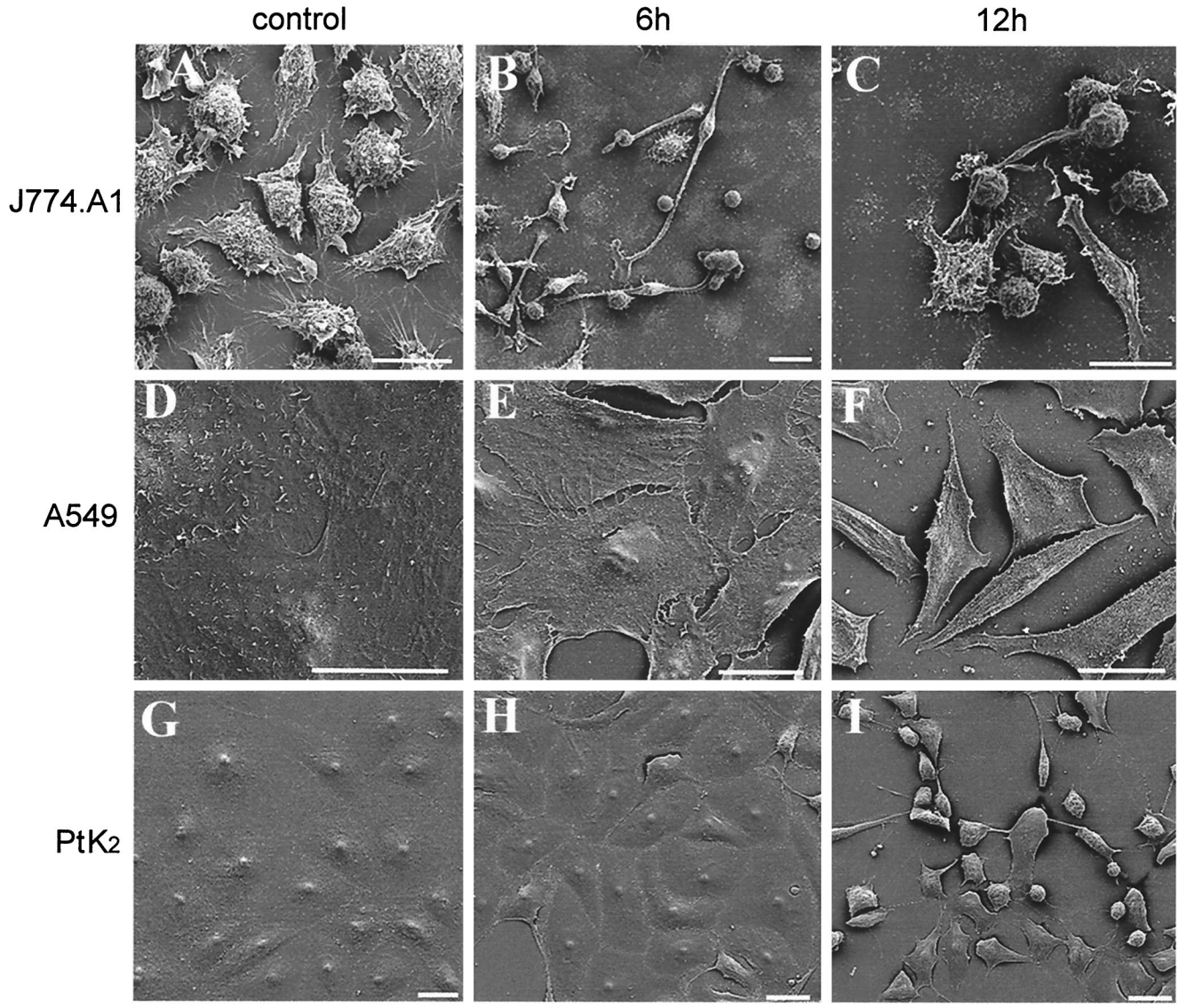

FIG. 1. Morphological changes induced by *B. pseudomallei* rhamnolipid. J774.A1 (A), A549 (D), and PtK_2 (G) control cells and cells exposed to *B. pseudomallei* rhamnolipid for 6 h (B, E, and H) and 12 h (C, F, and I) were observed by scanning electron microscopy. Rhamnolipid exposure led to a progressive rounding up and, finally, detachment in all three cell lines tested. Bar = 20 μm.

with rhamnolipid for 6 h and most stress fibers were concentrated in the cell periphery at this time point. Those peripheral stress fibers, which still contained myosin II (data not shown), became even more prominent after 12 h, whereas after 24 h most cells had contracted. In order to exclude the possibility that the observed morphological alterations were due to minor LPS impurities in our rhamnolipid preparations, we challenged PtK_2 cells with crude bacterial extracts, resulting in ~130 ng of *B. pseudomallei* LPS per ml. This LPS concentration was more than 10 times higher than the LPS concentration after exposure to the rhamnolipid preparation. However, no changes could be observed in the fluorescence-labeled actin cytoskeleton 6 h after exposure (data not shown), which indicated that the toxic effects of the rhamnolipid were not due to LPS contamination. Unlike the actin stress fibers, the microtubuli and the intermediate filament networks seemed to be unaffected following 6 h of rhamnolipid exposure (Fig. 2B and C). After 12 h of rhamnolipid exposure, the organization of the microtubules and the intermediate filaments was also affected (data not shown), due to the contraction of the cells.

Bacterial internalization is reduced in rhamnolipid-treated tissue-cultured macrophages. Because bacterial internalization is driven by the specific rearrangement of the actin cytoskeleton, we tested the phagocytic activity of the mouse macrophage cell line J774.A1. Compared to untreated controls, J774.A1 cells treated with rhamnolipid for only 3 h exhibited no morphological alterations but internalized significantly fewer viable *B. pseudomallei* E8 bacteria (Fig. 3).

***B. pseudomallei* rhamnolipid causes an impairment of cell cycle progression.** Microscopic observation of rhamnolipid-treated PtK_2, A549, and J774.A1 cells suggested that the toxin inhibits cell growth. We therefore used flow cytometric analysis

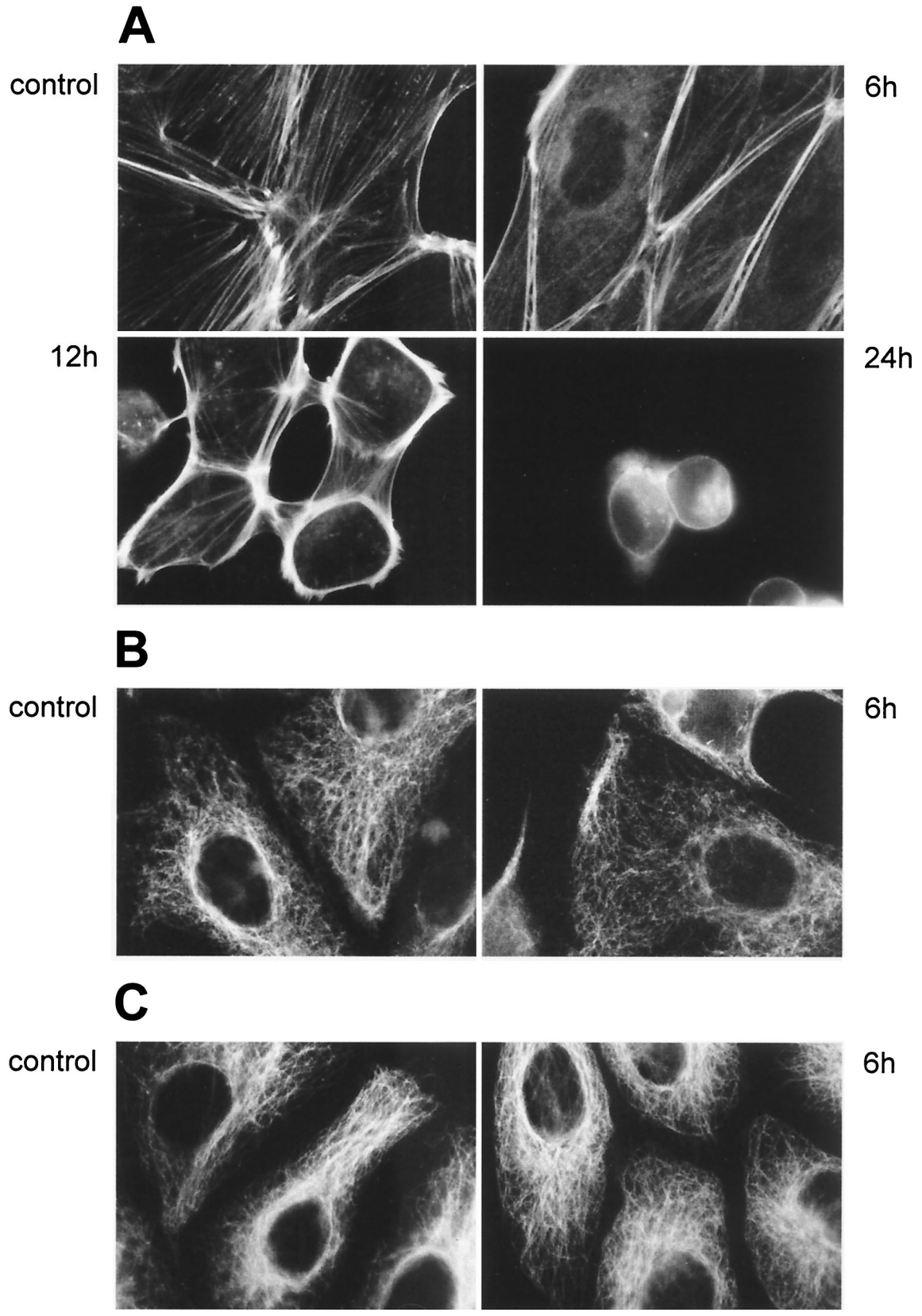

FIG. 2. Fluorescence microscopy of the cytoskeleton in rhamnolipid-treated cells. (A) Fluorescence-labeled filamentous actins of both control PtK_2 cells and cells exposed to *B. pseudomallei* rhamnolipid for 6, 12, and 24 h demonstrate a progressive reorganization of the actin network after intoxication. (B and C) Fluorescence-labeled intermediate (B) and microtubule (C) filaments in both control PtK_2 cells and cells exposed to rhamnolipid for 6 h. Rhamnolipid exposure did not seem to induce primary morphological changes in the microtubule and intermediate-filament networks.

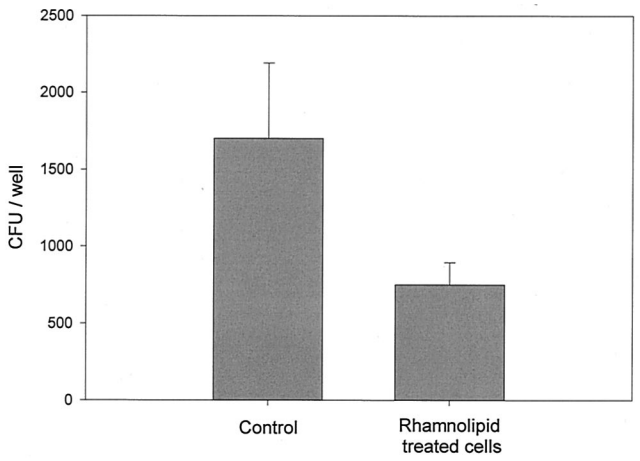

FIG. 3. Rhamnolipid treatment of J774.A1 cells led to a reduced uptake of viable *B. pseudomallei* bacteria. Control macrophages internalized significantly more bacteria within 30 min than cells treated with rhamnolipid for 3 h before infection (*t* test, $P = 0.001$). Data are the mean values (± SD) of results of one representative experiment performed in triplicate.

to determine whether the rhamnolipid had any effect on the cell cycle. In a serum-free-medium control, A549 and J774.A1 cells exhibited a profile typical of cycling cells, with 60.22% (standard deviation [SD], 8.81%) and 54% (SD, 11.1%), respectively, being in G_1, 5.69% (SD, 2.72%) and 5.11% (SD, 5.33%) being in G_2, and 34.1% (SD, 9.89%) and 40.91% (SD, 13.77%) being in S phase. After a 24-h exposure to only 1 μg of *B. pseudomallei* rhamnolipid per ml, which did not result in a detachment of the cells, we observed significant shifts in the A549 and J774.A1 cell populations, with 85.11% (SD, 7.23%) and 66.39% (SD, 17.76%), respectively, being in G_1 (paired *t* test; $P = 0.012$ and $P < 0.001$, respectively), 4.02% (SD, 1.18%) and 4.62% (SD, 4.39%) being in G_2 (paired *t* test; $P = 0.016$ and $P < 0.001$, respectively), and 10.87% (SD, 6.52%) and 28.99% (SD, 17.22%) being in S phase (differences were not significant). These data indicate that the toxin causes the cells to arrest in the G_0/G_1 phase of the cell cycle. In Fig. 4, a histogram from a representative flow cytometric experiment of the two cell lines is shown.

Conclusion. The actin cytoskeleton plays a fundamental role in eukaryotic cells, determining cell morphology and providing the driving force for dynamic processes such as cell motility,

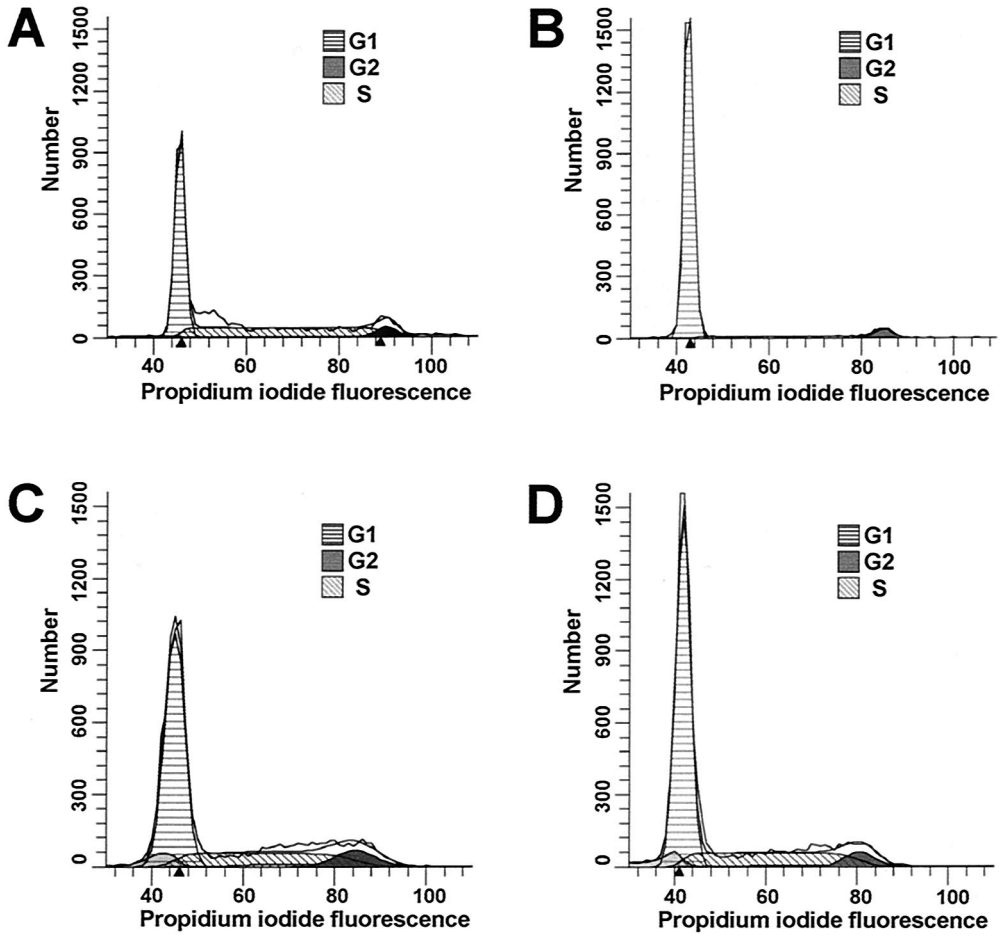

FIG. 4. Flow cytometry analysis revealed an impaired cell cycle progression in rhamnolipid-treated cells. Nuclei of control (A) and rhamnolipid-treated (B) A549 cells and of control (C) and rhamnolipid-treated (D) J774.A1 cells were isolated, stained with propidium iodide, and analyzed by flow cytometry. The data of one representative experiment are shown. In comparison to that of control cells, the number of rhamnolipid-treated cells in the G_0/G_1 phase of the cell cycle was increased, which indicated an impaired cell cycle progression.

phagocytosis, and growth (4, 10, 18). Our work demonstrates that *B. pseudomallei* rhamnolipid induced profound morphological alterations in various phagocytic and nonphagocytic cell lines. These alterations were apparently due to the reorganization of the cytoskeleton, characterized by the appearance of peripheral stress actin fibers and the loss of central stress fibers. Moreover, cellular functions such as phagocytosis were affected in rhamnolipid-treated cells, and an impaired cell cycle progression was observed. *B. pseudomallei* rhamnolipid is known to be produced at high bacterial densities in vitro (14), and *P. aeruginosa* rhamnolipid was detected in sputum samples of cystic fibrosis patients colonized with *P. aeruginosa* in the range of several micrograms per millliter of sputum (16). It therefore seems likely that the *B. pseudomallei* rhamnolipid concentrations used in this study are also present in vivo at time points of infection where high bacterial densities are encountered, e.g., in abscesses of the liver and spleen and in lungs during pneumonia.

There is growing evidence that the small GTPases (Rho, Rac, and Cdc42) play essential regulatory roles in alterations of the actin skeleton (13). While the activation of the GTPase Rho leads to stress fiber formation and is crucial for the regulation of cell cycle progression (23), the activation of Rac is characterized by a pronounced peripheral actin skeleton accompanied by the formation of lamellipodia and membrane ruffling (4, 13). The small GTPases not only are modulated by bacterial proteins (1) but also have been suggested to be a target for an extracellular mycolactone of *Mycobacterium ulcerans* (11, 12). This toxin exerts effects consistent with Rac activation and Rho inactivation, such as loss of stress fibers and pronounced peripheral actin staining. It also causes cell cycle arrest (11), which is very similar to the effects of the *B. pseudomallei* rhamnolipid described in this study. Further investigations should focus on the analysis of the primary target of the secreted *B. pseudomallei* rhamnolipid and the molecular mechanism that modulates the actin cytoskeleton, possibly via the small GTPases.

We thank Beate Sodeik and Katinka Döhner for valuable advice. We are especially grateful to Dieter Bitter-Suermann for his interest and strong support.

REFERENCES

1. **Aktories, K.** 1997. Rho proteins: targets for bacterial toxins. Trends Microbiol. **5:**282–288.
2. **Blose, S. H., D. I. Meltzer, and J. R. Feramisco.** 1984. 10-nm filaments are induced to collapse in living cells microinjected with monoclonal and polyclonal antibodies against tubulin. J. Cell Biol. **98:**847–858.
3. **Brett, P. J., and D. E. Woods.** 2000. Pathogenesis of and immunity to melioidosis. Acta Trop. **74:**201–210.
4. **Carpenter, C. L.** 2000. Actin cytoskeleton and cell signaling. Crit. Care Med. **28:**N94–N99.
5. **Chaowagul, W., Y. Suputtamongkol, D. A. Dance, A. Rajchanuvong, J. Pattara-arechachai, and N. J. White.** 1993. Relapse in melioidosis: incidence and risk factors. J. Infect. Dis. **168:** 1181–1185.
6. **Chaowagul, W., N. J. White, D. A. Dance, Y. Wattanagoon, P. Naigowit, T. M. Davis, S. Looareesuwan, and N. Pitakwatchara.** 1989. Melioidosis: a major cause of community-acquired septicemia in northeastern Thailand. J. Infect. Dis. **159:** 890–899.
7. **Dance, D. A., T. M. Davis, Y. Wattanagoon, W. Chaowagul, P. Saiphan, S. Looareesuwan, V. Wuthiekanun, and N. J. White.** 1989. Acute suppurative parotitis caused by Pseudomonas pseudomallei in children. J. Infect. Dis. **159:** 654–660.
8. **Dance, D. A. B.** 1991. Melioidosis: the tip of the iceberg? Clin. Microbiol. Rev. **4:**52–60.
9. **DeShazer, D., P. J. Brett, and D. E. Woods.** 1998. The type II O-antigenic polysaccharide moiety of Burkholderia pseudomallei lipopolysaccharide is required for serum resistance and virulence. Mol. Microbiol. **30:**1081–1100.
10. **Ernst, J. D.** 2000. Bacterial inhibition of phagocytosis. Cell Microbiol. **2:**379–386.
11. **George, K. M., L. P. Barker, D. M. Welty, and P. L. C. Small.** 1998. Partial purification and characterization of biological effects of a lipid toxin produced by *Mycobacterium ulcerans*. Infect. Immun. **66:**587–593.
12. **George, K. M., D. Chatterjee, G. Gunawardana, D. Welty, J. Hayman, R. Lee, and P. L. Small.** 1999. Mycolactone: a polyketide toxin from Mycobacterium ulcerans required for virulence. Science **283:**854–857.
13. **Hall, A.** 1998. Rho GTPases and the actin cytoskeleton. Science **279:**509–514.
14. **Häußler, S., M. Nimtz, T. Domke, V. Wray, and I. Steinmetz.** 1998. Purification and characterization of a cytotoxic exolipid of *Burkholderia pseudomallei*. Infect. Immun. **66:**1588–1593.
15. **Kouklis, P. D., A. Merdes, T. Papamarcaki, and S. D. Georgatos.** 1993. Transient arrest of 3T3 cells in mitosis and inhibition of nuclear lamin reassembly around chromatin induced by anti-vimentin antibodies. Eur. J. Cell Biol. **62:**224–236.
16. **Kownatzki, R., B. Tummler, and G. Doring.** 1987. Rhamnolipid of Pseudomonas aeruginosa in sputum of cystic fibrosis patients. Lancet **ii:**1026–1027.
17. **Leelarasamee, A., and S. Bovornkitti.** 1989. Melioidosis: review and update. Rev. Infect. Dis. **11:**413–425.
18. **May, R. C., and L. M. Machesky.** 2001. Phagocytosis and the actin cytoskeleton. J. Cell Sci. **114:**1061–1077.
19. **Ochsner, U. A., T. Hembach, and A. Fiechter.** 1996. Production of rhamnolipid biosurfactants. Adv. Biochem. Eng. Biotechnol. **53:**89–118.
20. **Reckseidler, S. L., D. DeShazer, P. A. Sokol, and D. E. Woods.** 2001. Detection of bacterial virulence genes by subtractive hybridization: identification of capsular polysaccharide of *Burkholderia pseudomallei* as a major virulence determinant. Infect. Immun. **69:**34–44.
21. **Steinmetz, I., M. Rohde, and B. Brenneke.** 1995. Purification and characterization of an exopolysaccharide of *Burkholderia* (*Pseudomonas*) *pseudomallei*. Infect. Immun. **63:**3959–3965.
22. **Suputtamongkol, Y., A. Rajchanuwong, W. Chaowagul, D. A. Dance, M. D. Smith, V. Wuthiekanun, A. L. Walsh, S. Pukrittayakamee, and N. J. White.** 1994. Ceftazidime vs. amoxicillin/clavulanate in the treatment of severe melioidosis. Clin. Infect. Dis. **19:** 846–853.
23. **Welsh, C. F., K. Roovers, J. Villanueva, Y. Liu, M. A. Schwartz, and R. K. Assoian.** 2001. Timing of cyclin D1 expression within G1 phase is controlled by Rho. Nat. Cell Biol. **3:**950–957.

Editor: B. B. Finlay